ISSN 1063-7745, Crystallography Reports, 2016, Vol. 61, No. 3, pp. 362–370. © Pleiades Publishing, Inc., 2016.
Original Russian Text © A.E. Blagov, Yu.A. Dyakova, M.V. Kovalchuk, V.G. Kohn, M.A. Marchenkova, Yu.V. Pisarevskiy, P.A. Prosekov, 2016, published in Kristallografiya, 2016, Vol. 61, No. 3, pp. 366–374.

DIFFRACTION AND SCATTERING OF IONIZING RADIATIONS

X-Ray Diffraction and X-Ray Standing-Wave Study of the Lead Stearate Film Structure

A. E. Blagov[a,b], Yu. A. Dyakova[a,b], M. V. Kovalchuk[a,b], V. G. Kohn[a,b], M. A. Marchenkova[a,b], Yu. V. Pisarevskiy [a,b], and P. A. Prosekov[a,b]

[a]*Shubnikov Institute of Crystallography, Russian Academy of Sciences, Leninskii pr. 59, Moscow, 119333 Russia*
[b]*National Research Centre "Kurchatov Institute", pl. Akademika Kurchatova 1, Moscow, 123182 Russia*
e-mail: prosekov@crys.ras.ru

Received November 27, 2015

Abstract—A new approach to the study of the structural quality of crystals is proposed. It is based on the use of X-ray standing-wave method without measuring secondary processes and considers the multiwave interaction of diffraction reflections corresponding to different harmonics of the same crystallographic reflection. A theory of multiwave X-ray diffraction is developed to calculate the rocking curves in the X-ray diffraction scheme under consideration for a long-period quasi-one-dimensional crystal. This phase-sensitive method is used to study the structure of a multilayer lead stearate film on a silicon substrate. Some specific structural features are revealed for the surface layer of the thin film, which are most likely due to the tilt of the upper layer molecules with respect to the external normal to the film surface.

DOI: 10.1134/S1063774516030044

INTRODUCTION

Currently, the study of organic films on solid substrates is of particular interest in view of the possibility of using them as components of hybrid systems. Organic molecules have various properties, because they perform all functions in living systems; at the same time, modern technologies provide many possibilities for the directed synthesis of these molecules. Inorganic materials are widely and successfully applied in different fields of industry, including electronics and acoustooptics, and their well-developed growth technology makes it possible to obtain crystals with high structural quality. Thus, hybrid systems based on a combination of organic materials and classical inorganic substrates are promising elements for various new-generation devices.

Organic films and crystals are generally characterized by large interplanar spacings. Correspondingly, special methods and approaches should be developed to study the structural characteristics of organic components. The functional properties of organic films are known to depend on the degree of their structural quality. Therefore, it is important to develop and adapt phase-sensitive methods for studying hybrid systems which could yield detailed information about small deviations of structure from periodicity.

In this paper we propose a method for studying crystal structure quality similar to the X-ray standing-wave method without measuring secondary processes [1–4], which uses multiwave interaction of diffracted beams corresponding to different harmonics of one reflection (i.e., different orders of reflection from one set of crystal planes).

Using the proposed adapted X-ray phase-sensitive method, we investigated a multilayer lead stearate film deposited on a silicon substrate by the Langmuir–Blodgett technique.

The Langmuir technique makes it possible to obtain periodic organic structures with a high degree of perfection on solid substrates while controlling the film deposition accurate to one monolayer. It is known that Langmuir lead stearate films can form a lamellar texture with a long axis oriented perpendicular to the substrate. In this case, the periodic arrangement of layers of lead ions along the normal to the substrate is observed with a high probability.

Our purpose was to analyze the possibility of applying the proposed method to study the real structure of thin organic films. In this paper we report the experimental conditions and measurement results, present the theory and calculation results, and discuss the data obtained.

SAMPLES

An organic film in the form of a periodic system composed of 80 lead stearate layers was formed on a silanized silicon substrate by the Langmuir–Blodgett technique. Lead stearate monolayers were obtained on the surface of aqueous subphase and transferred onto

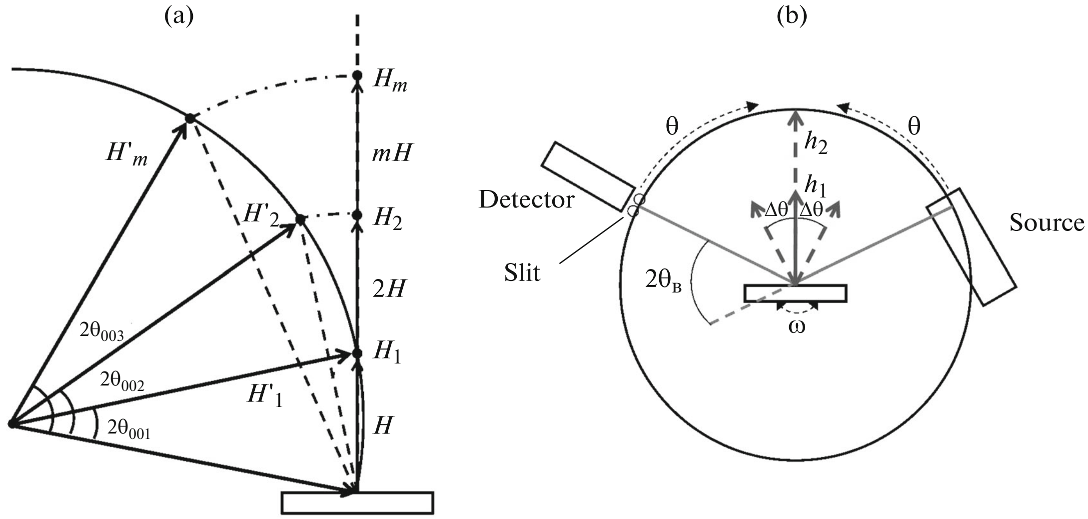

Fig. 1. Schematic of the scanning geometry in the reciprocal space used in the experiment: (a) Ewald construction and (b) X-ray diffraction scheme.

a solid substrate using a KSV 5000 system (KSV Instruments, Finland). The subphase was pure water (with a resistivity of 18 MΩ ·cm) prepared in a Simplicity 185 system (Millipore), with added $Pb(NO_3)_2$ in a concentration of 3×10^{-5} mol/L, pH = 7.2. The room temperature was maintained constant at a level of 20.0 ± 0.5°C. A solution of stearic acid in chloroform (concentration 0.7 mg/mL) was deposited on the aqueous subphase surface using a microliter syringe, after which the monolayer was compressed to a pressure of 25 mN/m using two symmetric mobile barriers. The thus formed monolayer was transferred onto a silanized (100)Si substrate. The substrate silanization was performed according to the procedure described in [5]. The samples for study were obtained using Si substrates with different roughnesses (no larger than 10 Å).

EXPERIMENTAL

The sample was studied by different X-ray methods and the X-ray standing-wave method at multiwave diffraction. Experiments were performed on an automatic SmartLab Rigaku X-ray diffractometer equipped with a 9-kW X-ray source with a rotating Cu anode.

In the first stage, $PbSt_2$ samples on Si substrates were studied by the X-ray reflectivity method in order to estimate the degree of structural quality of the structures fabricated and refine the parameters of their layer model (thickness, nonideality of interfaces, and depth homogeneity). Based on these data, structures of highest quality were selected for further study. Previously, methods for forming Langmuir–Blodgett films from $PbSt_2$ on Si substrates were developed when studying the thermal stability of these systems in [5]. Since the X-ray reflectivity curves reported in [5] are similar to our dependences, they are omitted here. It was also shown in [5] that these multilayer Langmuir films have a rather high structural quality and are thermally stable at temperatures comparable with room temperature (up to ~60°).

X-ray diffraction experiments were performed in the (+*n*–*m*) scheme of double-crystal X-ray diffraction in the horizontal geometry using a system of slits before the detector, which provided an angular resolution of 0.025°. The radiation from the source was collimated by a channel cut Ge monochromator with double 220 reflections, the X-ray characteristic line $CuK_{\alpha 1}$ was used. The beam transmitted through the monochromator was limited by a 0.05-mm slit (in the diffraction plane) installed before the sample. The diffracted X-ray intensity was recorded by a NaI detector.

The dependences of the reflections from the $PbSt_2$ film were recorded in both symmetric and asymmetric geometries. Different reflection orders from the planes parallel to the surface were used. The spacing between these planes was maximal and corresponded to the [001] direction, i.e., the *c* axis of the model unit cell.

Figure 1 shows schematically, using the Ewald construction (Fig. 1a), the experimental scanning geometry. During the measurements, the sample was fixed on a standard holder for studying plates, while the X-ray source and detector were rotated around a circle. The receiving slits made it possible to implement different angular scanning modes in the experiments, the so-called θ–2θ and ω scanning modes (Fig. 1b), which are widely used in high-resolution X-ray diffractometry [6].

The symmetric (strong) reflection was recorded using θ–2θ scanning in the direction of the $\mathbf{H}_m$ vector

(Fig. 1) in the vicinity of reciprocal lattice point H_m (m is the integer corresponding to the reflection order), i.e., in the narrow angular range near the Bragg angles of the $00l$-type reflections.

The asymmetric (weak) reflection was recorded by ω scanning along the $H'_m H_m$ arc (Fig. 1) practically perpendicular to the $\mathbf{H}_m$ vector at a small deviation from the reciprocal lattice point H_m; this situation also corresponds to angular deviation from the exact Bragg position for the $00l$ reflections, but at a fixed sum of the angle of incidence (θ_i) and the acceptance angle (θ_f), which is equal to the double Bragg angle of the reflection chosen.

Let us now consider the recording of a weak rocking curve by an example of (003) reflection. To measure the weak (003) reflection at the strong (001) reflection, the source is oriented at the Bragg angle of the (001) reflection, $\omega = \theta_i = \theta_{001}$, and the detector is oriented at the angle θ_f made by the reflected beam with the crystal surface, so that $\theta_f = 2\theta_{003} - \theta_{001}$, where θ_{003} is the Bragg angle of the (003) reflection. Then the rocking curve is measured as a function of angle ω in a narrow angular range near the Bragg angle of the strong (001) reflection.

This geometry of the experiment is simple and convenient: it can easily be adapted for any combination of strong and weak reflections of the ($00l$) type by choosing the corresponding angles for the source and detector orientations during scanning in the θ–2θ and ω modes. We investigated four different combinations of strong and weak reflections: (001, 002), (001, 003), (002, 003), and (003, 002). The total analysis of all cases yields much more information than any single case; in particular, one can draw a more accurate conclusion about the displacement of atomic layers near the surface.

Since the interplanar spacing along the diffraction vector (d = 50 Å) exceeds the Cu$K_{\alpha1}$ wavelength (λ = 1.54 Å) greatly, the Bragg angle for the first-order reflection is small: $\theta_{001} = 0.8827°$. The small value of this angle, on the one hand, increases the reflection amplitude for a unit length along the normal to the film surface. On the other hand, it reduces the difference of the Bragg angles between neighboring reflection orders.

In view of the aforesaid, the angular width of reflections increases. Due to this, one can record a very weak asymmetric diffraction into a neighboring-order reflection, for example, (002), if the Bragg condition is satisfied for the main reflection (e.g. (001)). If the reflection occurs simultaneously into several beams, one deals with a special case of multiwave diffraction, in which the diffraction into the strong reflection is rather high and is implemented dynamically, whereas the diffraction into weak reflections occurs kinematically but with formation of an X-ray standing wave (**XSW**) in the crystal.

This case was described in [1–4] and referred to as the *X-ray standing-wave method without secondary radiation*. To experimentally implement this method for typical perfect crystals (with lattice parameters ~5 Å, for example, Si, Ge, GaAs, etc.), one must specially orient a crystal under study by rotating it around two axes [7, 8]. Under these conditions, one always uses the reflections whose reciprocal lattice vectors make some angle. Here, this method is implemented for the first time for parallel reciprocal lattice vectors corresponding to different orders of a set of ($00l$) reflections.

A weak reflection is known to stem from a thin surface layer of crystal and be affected by the phase of the strong reflection amplitude. For this reason, the rocking curves always have an asymmetric character of a dispersion curve with a minimum and a maximum at both sides from the center of the strong reflection. If the planes in the surface layer are displaced with respect to their position in the ideal crystal lattice, this displacement directly manifests itself in the angular dependence of weak reflection and can be determined by comparison with the results of numerical calculation.

This feature of the XSW method was theoretically discussed for the first time in [9] and described in detail in review [10]. The use of the new modification of the XSW method for Langmuir lead stearate films makes it possible to study the structure of the film surface layer without a complex alignment of the crystal and use different combinations of strong and weak reflections from an immobile sample.

Some multilayer structures, including Langmuir films on solid substrates, were investigated in [11–13]. Note that the possibility of multiwave X-ray interaction was disregarded in these studies, and they were aimed mainly at determining the influence of surface roughness on the main reflection.

Despite the fact that the weak-reflection intensity is fairly low in comparison with the strong reflection, it could be measured using a laboratory X-ray source. Hence, this method can be widely used to study Langmuir films of different types.

RESULTS

Figure 2 shows the angular dependences of the reflections recorded for the first two cases. Strong reflection 001, weak reflection 002, and weak reflection 003 are presented in panels a, b, and c, respectively. One can see that the number of photons is insufficient for measuring the third curve, as a result of which the statistical noise is pronounced. However, one can conclude that the asymmetry of the 003 reflection curve has the same sign as in the case of reflection 002. Note also that the asymmetry of the weak reflection curves is incomplete: the minimum is much weaker than the maximum.

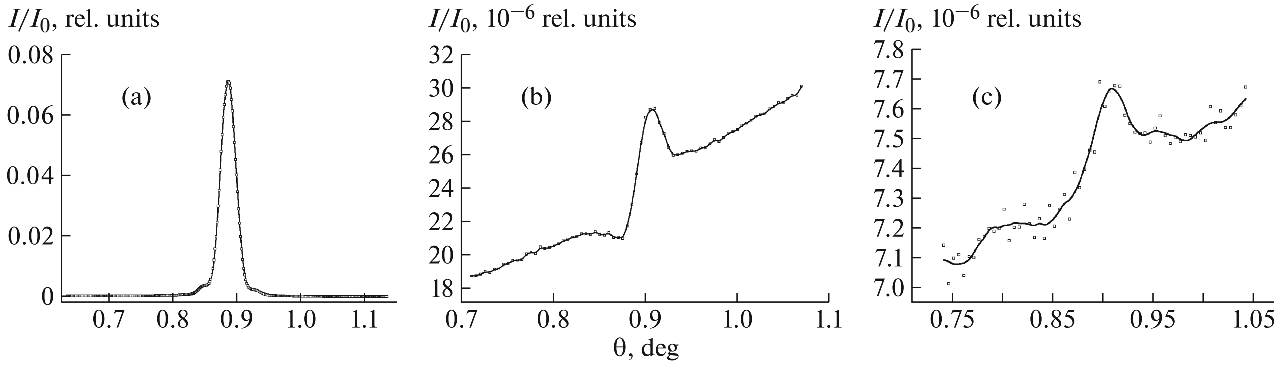

Fig. 2. Experimental dependences of diffraction reflections from a multilayer lead stearate film: (a) symmetric reflection 001 and (b, c) weak asymmetric reflections 002 and 003, respectively, near the Bragg position for the 001 reflection.

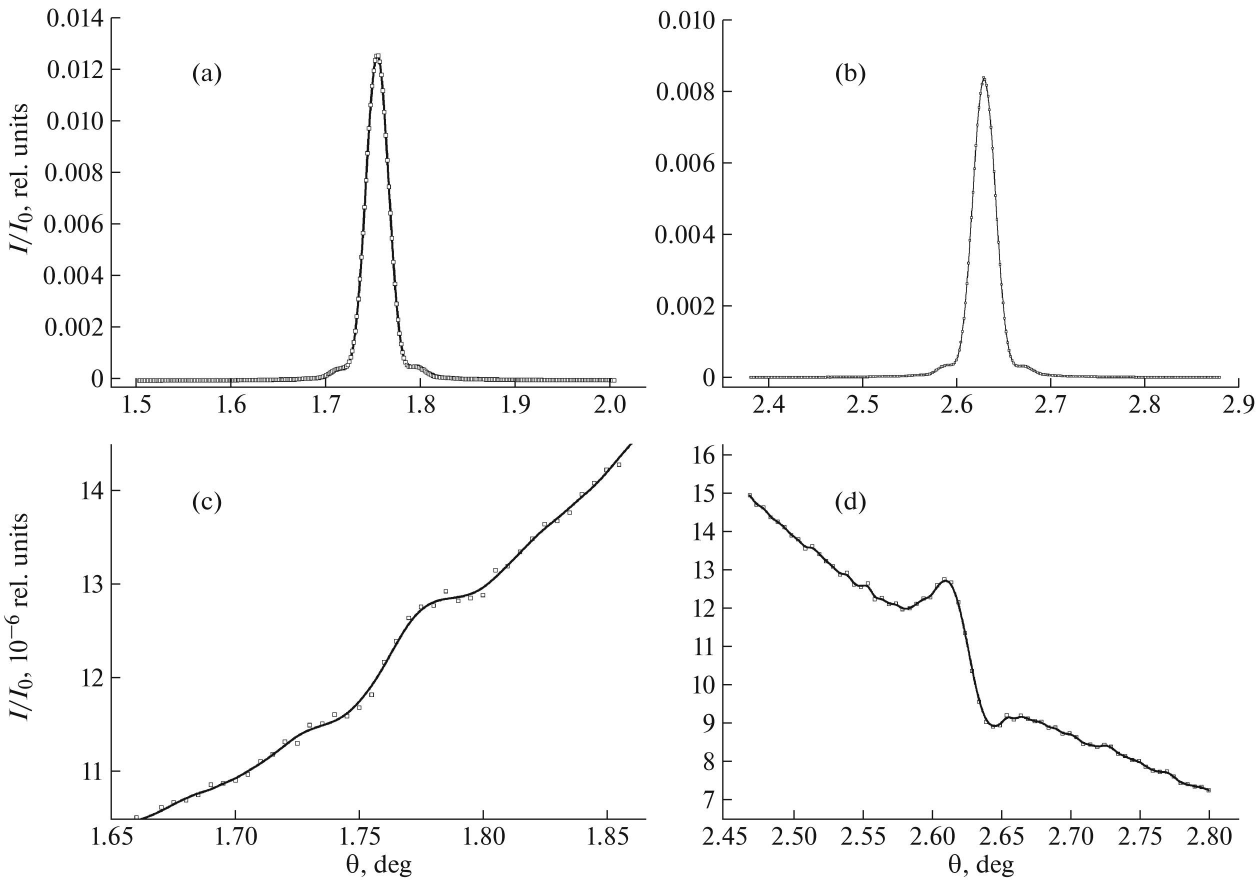

Fig. 3. Experimental dependences of diffraction reflections from a multilayer lead stearate film: (a, b) the symmetric 002 and 003 reflections, respectively, and (c, d) weak asymmetric 003 and 002 reflections near the Bragg positions for the 002 and 003 reflections, respectively.

Figure 3 shows the curves for the last two cases. Two strong 002 and 003 reflections are presented in Fig. 3a and Figs. 3b, the weak 003 and 002 reflections are shown in Fig. 3c and Fig. 3d, respectively. An interesting fact is that weak-reflection curve for the third case has a very weak dispersion, whereas the similar curve for the fourth case has a dispersion opposite that observed for the first case: the maximum is on the left and the minimum is on the right.

THEORY

The Bragg diffraction of X rays occurs in any object with a periodic change in electron density if the Bragg condition $2d\sin\theta = m\lambda$ (d is the period; λ is the radiation wavelength; and m is an integer, referred to as the reflection order) is satisfied. Having entered a crystal, a plane wave generates a set of new plane waves whose wave vectors differ by reciprocal lattice vectors. If the wave vector of the incident wave is $\mathbf{k}_0$, additional plane waves with wave vectors $\mathbf{k}_m = \mathbf{k}_0 + \mathbf{h}_m$, where $\mathbf{h}_m$ is the reciprocal lattice vector with a number m, can be generated.

The Bragg condition is equivalent to the elastic scattering condition when the moduli of the wave vectors of the incident and reflected waves are equal: $|\mathbf{k}_m|^2 = |\mathbf{k}_0|^2$. In a long-period quasi-one-dimensional crystal, one can select a set of reciprocal lattice vectors with identical directions but different moduli corresponding to different reflection orders $\mathbf{h}_m = mh\mathbf{n}$, where $\mathbf{n}$ is the unit vector along the period direction. In the case under consideration, it coincides with the direction of external normal to the crystal surface; $h = 2\pi/c$ (c is the crystal period in the chosen direction) and $m = \pm1, \pm2$, etc.

The Bragg condition cannot be satisfied exactly for two reciprocal lattice vectors with different m values. However, there may be a situation where the Bragg condition is satisfied well for one reflection order and poorly for another order. This situation is not implemented in conventional three-dimensional crystals, because their lattice period is approximately equal to the X-ray wavelength. Nevertheless, it may occur in multilayer long-period (for example, organic) structures in which Bragg angles are small and the angular distance from one reflection order to another is small as well.

Three-wave diffraction in a one-dimensional structure is coplanar; i.e., all plane-wave vectors lie in the same plane. In this case, the unit polarization vectors of the electric field can be chosen so as to provide the existence of two systems of noninteracting waves. However, if the diffraction angles are small, that radiation polarization barely changes and affects the observed angular dependence curves only slightly. Therefore, one can approximately consider the scalar amplitudes of the radiation electric field.

It is known that, in the case of very small diffraction angles (comparable with the total external reflection angle), one must take into account specularly reflected waves. Let the diffraction angles be large enough to neglect the influence of specularly reflected waves. We will consider a three-wave case where an incident wave with a wave vector $\mathbf{k}_0$, being reflected generates a strong wave with a wave vector $\mathbf{k}_n$ and a weak wave with a wave vector $\mathbf{k}_m$.

If all three waves are formally considered strong, the equations for their scalar amplitudes take the form [14]

$$\begin{aligned}(\alpha_0 + 2\varepsilon\gamma_0)E_0 &= X_{00}E_0 + X_{0n}E_n + X_{0m}E_m,\\ (\alpha_n + 2\varepsilon\gamma_n)E_n &= X_{n0}E_0 + X_{00}E_n + X_{nm}E_m,\\ (\alpha_m + 2\varepsilon\gamma_m)E_m &= X_{m0}E_0 + X_{mn}E_n + X_{00}E_m\end{aligned} \tag{1}$$

Here it is assumed that the wave vectors in the crystal, being refracted, get an additive $-K\varepsilon\mathbf{n}$, $K = 2\pi/\lambda$, $\gamma_0 = k_{0z}/K = \sin(\theta_B)$ (the z axis is directed antiparallel to $\mathbf{n}$), $\gamma_n = k_{nz}/K$, $\gamma_m = k_{mz}/K$, $\alpha_0 = 0$,

$$\alpha_n = (\mathbf{k}_0 + \mathbf{h}_n)^2/K^2 - 1 = -2\sin(2\theta_B)\Delta\theta, \tag{2}$$

$$\begin{gathered}X_{ij} = -\frac{\lambda^2 r_0}{\pi V_0}F(\mathbf{k}_i - \mathbf{k}_j),\\ F(\mathbf{h}) = \sum_k f_k(\mathbf{h})W_k(\mathbf{h})\sum_{l=1}^{l_k}\exp(i\mathbf{h}\mathbf{r}_{lk}).\end{gathered} \tag{3}$$

Here the subscripts i and j take values of 0, n, and m; V_0 is the volume of crystal unit cell; $r_0 = e^2/mc^2$ is the classical electron radius; and $F(\mathbf{h})$ is the Fourier transform of electron density in the unit cell. A calculation starts with selection of a group of identical atoms, which are enumerated by subscript k. The Fourier component of electron density, $f_k(\mathbf{h})$, and Debye–Waller factor $W_k(\mathbf{h})$ for an individual atom are identical in this group. However, the atoms differ in geometric position, which is taken into account by the second sum over l, where $\mathbf{r}_{lk}$ is the coordinate of the lth atom in the kth group.

Angle $\Delta\theta$ is assumed to be small; it is chosen so as to make the total angle be $\theta = \theta_n + \Delta\theta$, where θ_n is the Bragg angle for the nth reflection. It is noteworthy that parameter α_m is not arbitrary in this case, because the sample is not rotated and has not an additional degree of freedom. This parameter must be expressed in terms of α_n.

Let us demonstrate this simple calculation by an example of $n = 001$ and $m = 002$. In this case, $\mathbf{h}_m = 2\mathbf{h}_n$. Therefore,

$$\begin{aligned}\alpha_m &= (\mathbf{k}_0 + 2\mathbf{h}_n)^2/K^2 - 1 = (4\mathbf{k}_0\mathbf{h}_n + 4h_n^2)/K^2\\ &= 2\alpha_n + 2h_n^2/K^2 = 2\alpha_n + 8\gamma_0^2.\end{aligned} \tag{4}$$

Here we use the relation $h_n = 2K\gamma_0$. The formulas for the other three cases can be obtained in the same way:

$$\begin{gathered}(n = 001, m = 003)\,\alpha_m = 3\alpha_n + 48\gamma_0^2,\\ (n = 002, m = 003)\,\alpha_m = (3/2)\,\alpha_n + 3\gamma_0^2,\\ (n = 003, m = 002)\,a_m = (2/3)\,a_n - (8/9)\,\gamma_0^2.\end{gathered} \tag{5}$$

Parameter γ_0 in each formula corresponds to the Bragg angle for the strong reflection; therefore, it has different values.

It follows from (5) that α_n may be close to zero, while the α_m value is always large in comparison with X_0. Correspondingly, the E_m value is much smaller than E_0 and E_n and it can be calculated within the perturbation theory, neglecting the influence of the weak value on the strong ones. First, we will consider the first two equations of system (1) without the term containing E_m:

$$2\varepsilon\gamma_0 E_0 = X_{00}E_0 + X_{0n}E_n,$$
$$(\alpha_n + 2\varepsilon\gamma_n)E_n = X_{n0}E_0 + X_{00}E_n. \quad (6)$$

This system has a solution only if its determinant is zero. This condition yields the equation for parameter ε:

$$(X_{00} - 2\varepsilon\gamma_0)(X_{00} - 2\varepsilon\gamma_n - \alpha_n) = X_{n0}X_{0n}. \quad (7)$$

The solutions to this equation and the amplitude ratios have the form

$$2\varepsilon_{1,2} = x_0 + x_n \pm \left(x^2 + (x_0 - x_n)^2\right)^{1/2},$$
$$R_{1,2} = \frac{E_n}{E_0} = \frac{2\varepsilon_{1,2}\gamma_0 - X_{00}}{X_{0n}}, \quad (8)$$

where $x_0 = X_{00}/2\gamma_0$, $x_n = (X_{00} - \alpha_n)/2\gamma_n$, $x^2 = X_{n0}X_{0n}/\gamma_0\gamma_n$. For the second diffracted wave, the amplitude ratio is obtained from the third equation of system (1):

$$F_{1,2} = \frac{E_m}{E_0} = \frac{X_{m0} + X_{mn}R_{1,2}}{\alpha_m + 2\varepsilon_{1,2}\gamma_m - X_{00}}. \quad (9)$$

The above theory suggests that the crystal is perfect. If the crystal is deformed or partially damaged, one must consider a more complex theory in which the diffraction in different parts of crystal occurs differently. This more complex theory, in particular, introduces into consideration the concept of thickness of the surface layer in which efficient reflection occurs.

If the Bragg condition is exactly fulfilled, total reflection arises only when the crystal thickness exceeds extinction length L_{ex}, which is defined as [15]

$$L_{ex} = \frac{\lambda(\gamma_0|\gamma_n|)^{1/2}}{\pi\,\mathrm{Re}(X_{0n}X_{n0})^{1/2}}. \quad (10)$$

For a weak reflection, Bragg condition is satisfied poorly because $|\alpha_m| \gg X_{00}$. One can show that in this case only a thin surface layer of crystal is involved in reflection; the thickness of this layer is approximately

$$L = \frac{\lambda(\gamma_0|\gamma_m|)^{1/2}}{\pi|\alpha_m|}. \quad (11)$$

The information about the thickness of the crystal surface layer from which reflection occurs is valuable to take into account the peculiar defect structure of crystal, which is in the following. Let the crystal lattice be perfect in deeper layers. Then the strong reflection is formed in these layers and the X-ray standing wave in the crystal has a periodicity of these layers.

However, the external layer, to which the weak reflection with subscript m corresponds, can be shifted along the normal to the surface from the position that it would have in a perfect crystal. If the displacement is u, it can be taken into account by slightly changing formula (9), as was shown in [1, 10]:

$$F_{1,2} = \frac{E_m}{E_0} = \frac{X_{m0} + X_{mn}R_{1,2}\exp(i\varphi_n)}{\alpha_m + 2\varepsilon_{1,2}\gamma_m - X_{00}}, \quad \varphi_n = hun. \quad (12)$$

Additional phase φ_n is introduced in complete analogy with the theory of XSW method [9, 10].

Since there are two solutions, the total field is their superposition with coefficients $a_{1,2}$, which determine the degree of excitation of each solution. They are found from the boundary conditions for strong waves:

$$a_1 + a_2 = 1, \quad a_1R_1C_1 + a_2R_2C_2 = 0,$$
$$C_{1,2} = \exp\left(iK\varepsilon_{1,2}T\right), \quad (13)$$

where T is the crystal thickness.

The solution to this system has the form

$$a_1 = \frac{1}{1 - R_1C_1(R_2C_2)^{-1}},$$
$$a_2 = 1 - a_1 = -\frac{R_1C_1(R_2C_2)^{-1}}{1 - R_1C_1(R_2C_2)^{-1}}. \quad (14)$$

Respectively, the strong-reflection amplitude is

$$B_n = a_1R_1 + a_2R_2 = \frac{R_1R_2(C_2 - C_1)}{R_2C_2 - R_1C_1}. \quad (15)$$

It follows from (8) that $R_1R_2 = -(\gamma_0/\gamma_n)(X_{n0}/X_{0n})$. If $X_{n0} = X_{0n}$ and $\gamma_n = -\gamma_0$, $R_1R_2 = 1$. The reflection coefficient for the second reflection is $B_m = a_1F_1 + a_2F_2$ (functions F_1 and F_2 were defined in (12)).

Note that, if $|\alpha_m| \gg 2|\varepsilon\gamma_m|$, X_{00}, weak corrections can be neglected in the first approximation. Then B_m can easily be expressed in terms of B_n:

$$B_m = \frac{X_{m0} + X_{mn}B_n\exp(i\varphi)}{\alpha_m}. \quad (16)$$

This approximate formula explains the form of the angular dependence for the weak reflection. Far from the region of the first strong reflection, coefficient B_n is close to zero; thus, we have an almost constant reflection, which changes weakly and monotonically with a change in parameter α_m.

However, the second term in the numerator of formula (16) plays an important role in the region of the first strong reflection. The real part of complex coefficient B_n is known to change sign at the center of the reflection region and have different signs at its boundaries. Specifically for this reason the angular dependence takes a dispersion form. The presence of an additional phase factor changes the form of the dispersion curve.

DISCUSSION

Based on an analysis of the compression isotherm and the structural data in the literature, we constructed a unit-cell model (Fig. 4a). The lead stearate unit cell is known to be pseudo-orthorhombic (monoclinic, with angles close to 90°) [16]. Hydrocarbon

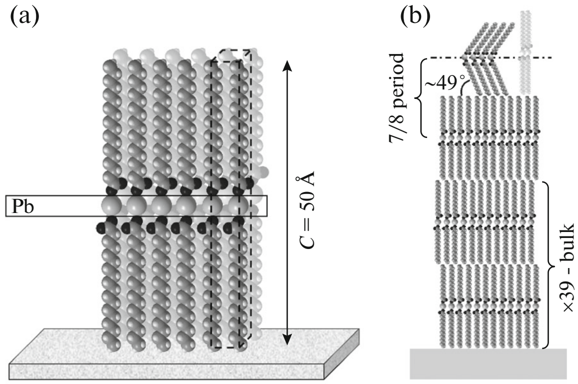

Fig. 4. (a) Model of the unit cell of a lead stearate film on a solid substrate and (b) the model of a multilayer periodic lead stearate film. The change in the structure of the surface layer of multilayer film, caused by the inclination of the upper layer molecules with respect to the external normal to the film surface, is schematically shown.

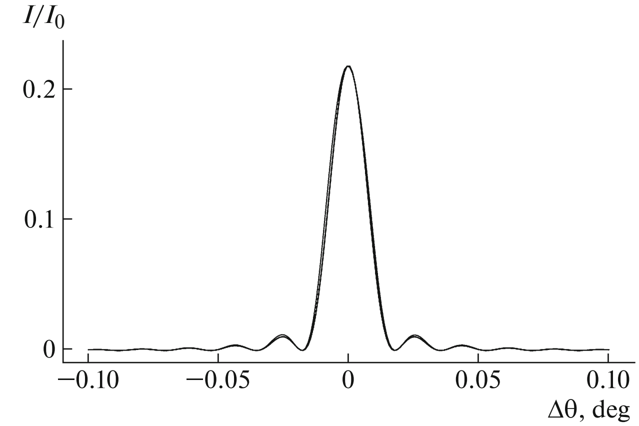

Fig. 5. Theoretical dependences of the diffraction reflection coefficient of a multilayer lead stearate film for strong symmetric 001, 002, and 003 reflections.

chains are oriented perpendicular to the substrate plane and the unit-cell parameters may slightly vary depending on the film formation conditions [17]. The experiment aimed at determining the double angle of diffraction reflection 001 revealed that parameter c = 50 Å under chosen conditions of lead stearate film deposition. The crystal has 40 periods; thus, it is a multilayer film with a thickness of about 2000 Å (Fig. 4b).

The chemical formula of lead stearate is $(CH_3(CH_2)_{16}COO)_2Pb$; correspondingly, the crystal has 111 atoms per unit cell. The model atomic coordinates in the unit cell were used to calculate the structural factors describing the phase relations in the case of X-ray scattering by a single unit cell.

The formulas described in the previous section were used to calculate the theoretical curves of diffraction reflection coefficient in the strong and weak reflections for all four experimental configurations. The curves are relatively wide; therefore, the incident beam can be considered flat and monochromatic, because the width of the spectral line Cu$K_{\alpha 1}$ of X-ray tube and the angular range of crystal reflection are small in comparison with the diffraction reflection coefficient curve.

For this reason, the calculation was performed in the approximation of the incident plane monochromatic wave. The Fourier components of polarizability (diffraction parameters) were calculated using the program described in [18]. It is noteworthy that the crystal does not have a center of symmetry and the replacement of X_{n0} with X_{0n} and vice versa may lead to different results. However, it turned out that the real parts differ only slightly, while the imaginary parts do not affect the result. Figure 5 shows the calculated curves of diffraction reflection coefficient for the strong reflections 001, 002, and 003. The 001 curve is shown as it is, while the 002 and 003 curves are multiplied by factors of 4.56 and 8.92, respectively, to make the peak values of the curves coincide. As follows from Fig. 5, the shape of the curves for all reflections changes only slightly, as one would expect, because the film thickness is smaller than the extinction length (10).

Figure 6 shows the curves of diffraction reflection coefficient in weak reflections for all four experimental configurations. The designation of the vertical axis in the four fragments is as follows: the subscript indicates a weak reflection and the superscript indicates a strong reflection. The bold lines are the curves calculated taking into account the additional phase (i.e., using formula (12)), and the thin lines are the curves calculated for an ideal crystal (from formula (9)).

A comparison of the theoretical and experimental data shows that the experimental curves are nevertheless broadened and distorted by instrumental function; however, this distortion is insignificant. In particular, the half-width of the strong reflection 001 in the experimental curve is 0.03°, whereas the half-width of the theoretical curve is 0.02°. One can easily see that the consideration of additional phase significantly improves the agreement between calculated and experimental curves. In the cases of 002 (001), 003 (001), and 003 (002), the curve dispersion sign is the same both for the phase taken into account and for the ideal film. However, the shape of the curve with phase taken into consideration is much closer to the experimental curve.

It is of interest that, for the 002 (003) combination, considering the phase makes it possible to correctly describe the dispersion of the curve, which is close to experimental; at the same time, it has opposite sign for the ideal crystal. In the above designation, the weak reflection stands first, while the strong reflection is in parentheses. Thus, a comparison of experimental

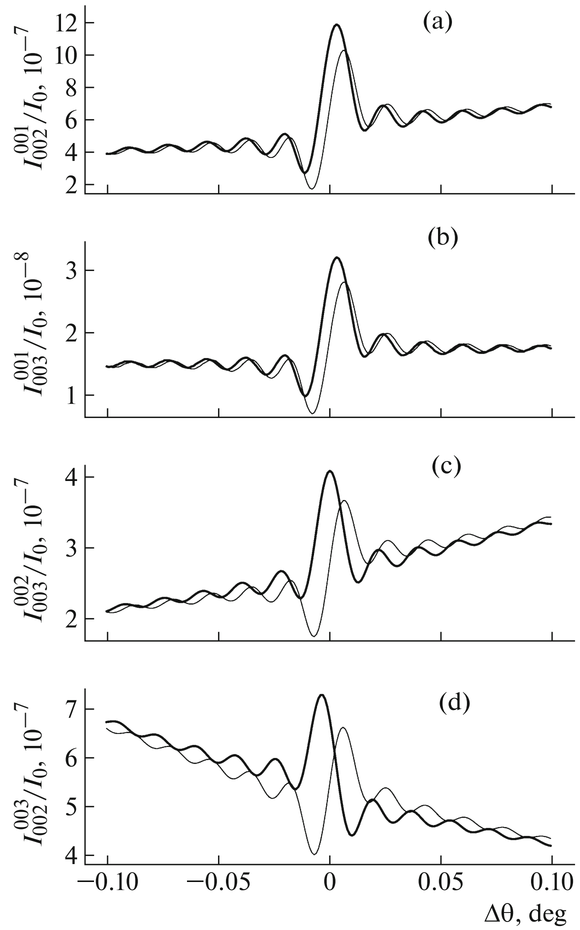

Fig. 6. Theoretical dependences of the diffraction reflection coefficient of a multilayer lead stearate film for weak asymmetric 002 (001), 003 (001), 003 (002), and 002 (003) reflections. A weak reflection stands first in designations, and the strong reflection (near the Bragg position of which the dependence is shown) is in parentheses.

curves with calculated ones shows that the film obtained is not ideal but strained. One can estimate only the surface layer strain, to which weak reflection curves indicate. Strong reflection curves do not contain such information.

A comparison of the results suggests that the layer of lead ions in the film surface region, being averaged over the zone exposed to the X-ray beam, is shifted along the vertical axis so that an additional phase ($\pi/4$) arises for the 001 reflection. In other words, the displacement is $u = c/8$ along the external normal direction. The displacement is determined accurate to the lattice constant; therefore, another possible version is $u = -7c/8$. The phases for the 002 and 003 reflections are, respectively, $\pi/2$ and $-3\pi/4$.

This shift of lead ions in the surface layers can be explained in one of two ways. First, the film surface is inhomogeneous in the lateral plane; i.e., there is roughness comparable with the lead stearate bilayer thickness. The hydrophobic tails of the last lead stearate layer make an angle of 40° with the external normal to the surface (the angle between the hydrophobic tails of molecules and the substrate is 50°, as is shown in Fig. 4b). However, the high roughness of the upper layer would lead to a change in the dispersion curve profile with a change in the sample area exposed to the X-ray beam; however, this was not observed experimentally. The second (most likely) reason is the inclination of lead stearate molecules at the bulk sample—air interface. The angle between lead stearate hydrocarbon tails in the upper-layer model presented in Fig. 4b corresponds to the approximation of a single molecule located beyond the crystal. Thus, one can conclude that the surface-layer structure differs from the structure of the layers in the film bulk.

A signal averaged over the exposed area was recorded in our experiment. Therefore, an additional study must be performed to unambiguously determine the mechanism of deterioration of the structural quality of surface layers in the case under consideration

Note also that the theory cannot explain the almost complete disappearance of dispersion in the weak reflection curve for the 002 (003) combination. At a phase of $\pi/2$, the real part of amplitude B_m in formula (16) does not contribute to the curve; however, there is a contribution from the imaginary part. Correspondingly, the calculated curve is symmetric, but the deviation of the maximum from the background is rather large. The cause of this discrepancy is unclear and calls for additional study.

ACKNOWLEDGMENTS

We are grateful to E.Yu. Tereshchenko (Institute of Crystallography, Russian Academy of Sciences) and S.N. Yakunin (National Research Centre "Kurchatov Institute") for the discussion of the results and fruitful advice and remarks.

This study was performed using the equipment of the Mixed-Use Center "Structural Diagnostics of Materials" of the Institute of Crystallography, Russian Academy of Sciences, and supported in part by the Russian Foundation for Basic Research, project nos. 15-29-01142 ofi_m, 14-22-01042 ofi_m, 16-32-60120 mol_a_dk, and 16-32-60144 mol_a_dk.

REFERENCES

1. V. G. Kohn, Phys. Status Solidi A **106** (1), 31 (1988).
2. V. G. Kohn, J. Moscow Phys. Soc. **1** (4), 425 (1991).
3. V. G. Kohn and L. V. Samoilova, Phys. Status Solidi A **133** (1) (1992).
4. A. Yu. Kazimirov, M. V. Koval'chuk, and V. G. Kohn, Kristallografiya **39** (2), 258 (1994).
5. M. A. Marchenkova, Yu. A. D'yakova, A. Yu. Seregin, et al., Poverkhnost, No. **11**, 1 (2013).

6. V. Holy, U. Pietsch, and T. Baumbach, *High-Resolution X-Ray Scattering from Thin Films and Multilayers. Springer Tracts in Modern Physics* (Springer, Berlin, 1999), Vol. 149, Pt. I, p. 31.

7. M. V. Kovalchuk, A. Kazimirov, V. Kohn, et al., Phys. B: Condens. Matter **221**, 445 (1996).

8. A. Yu. Kazimirov, M. V. Kovalchuk, I. Yu. Kharitonov, et al., Rev. Sci. Instrum. **63**, 1019 (1992).

9. A. M. Afanas'ev and V. G. Kohn, Zh. Eksp. Teor. Fiz. **74** (1), 300 (1978).

10. M. V. Koval'chuk and V. G. Kohn, Usp. Fiz. Nauk **149** (1), 69 (1986).

11. D. E. Savage, J. Kleiner, N. Schimke, et al., J. Appl. Phys. **69** (3), 1411 (1991).

12. V. Nitz, M. Tolan, J.-P. Schlomka, et al., Phys. Rev. B **54** (7), 5038 (1996).

13. V. M. Kaganer, S. A. Stepanov, and R. Kohler, Phys. Rev. B **52** (23), 16369 (1995).

14. Z. G. Pinsker, *X-ray Crystal Optics* (Nauka, Moscow, 1982) [in Russian].

15. V. G. Kohn, Phys. Status Solidi B **231** (1), 132 (2002).

16. V. V. Klechkovskaya and L. A. Feigin, Kristallografiya **43** (6), 975 (1998).

17. J. B. Peng, G. T. Barnes, and I. R. Gentle, Adv. Colloid Interface Sci. **91**, 163 (2001).

18. V. G. Kohn, Crystallogr. Rep. **51** (6), 936 (2006).

Translated by Yu. Sin'kov